Electronic Supplementary Material

Symmetry-Breaking-Induced Ferroelectric HfSnX₃ Monolayers and their Tunable Janus Structures: Promising Candidates for Photocatalysts and Nanoelectronics

Yu Zhang [a], Yanqing Shen [a,b],* , Jiajia Liu [a], Lingling Lv [a] , Min Zhou [a], Xin Yang [a],

Xianghui Meng [a], Bing Zhang [a], Zhongxiang Zhou [a,b],*

[a]School of Physics, Harbin Institute of Technology, Harbin, 150001, PR China

[b]Heilongjiang Provincial Key Laboratory of Plasma Physics and Application Technology, Harbin Institute of Technology, Harbin 150001, PR China

*Corresponding authors: Yanqing Shen, E-mail: shenyanqing2004@163.com

Zhongxiang Zhou, E-mail: zhouzx@hit.edu.cn
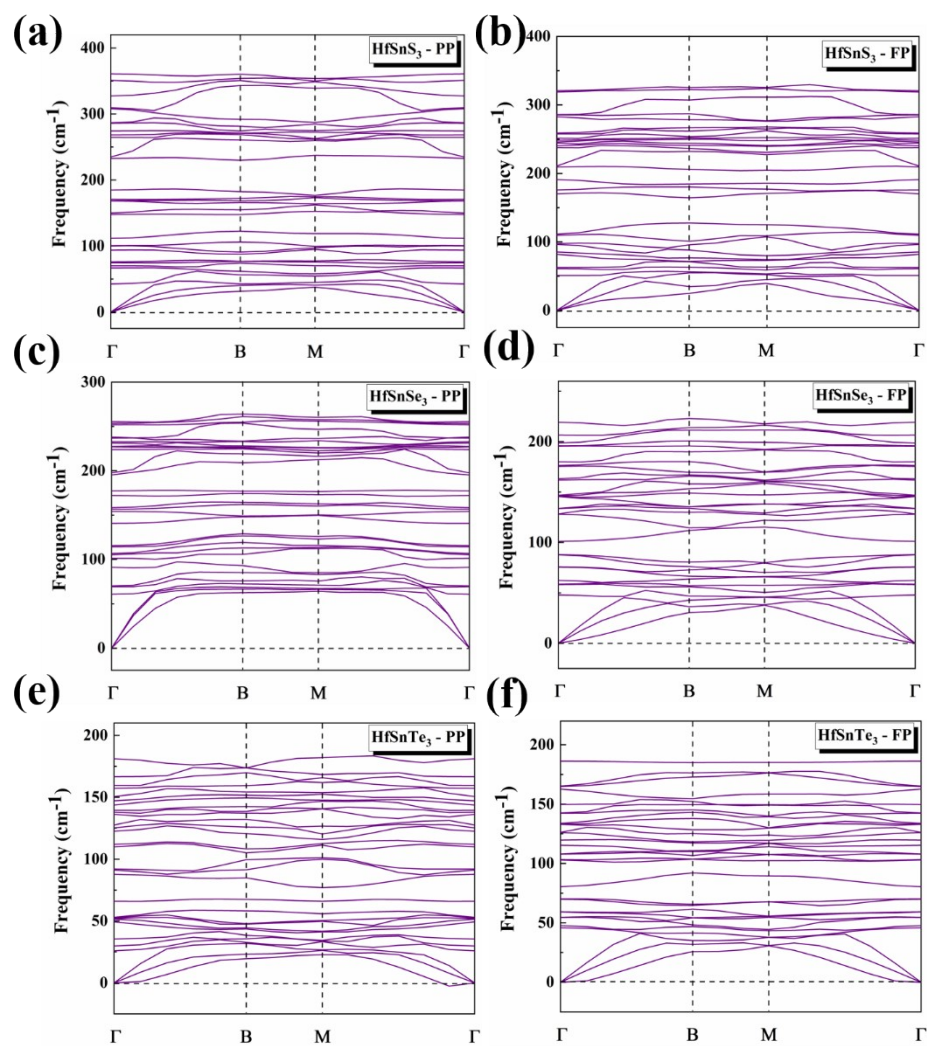
Supplementary Material

Fig. S1. Phonon spectrum of PP and FP HfSnX$_3$ monolayers. (a) and (b) represent the HfSnS$_3$ monolayers, (c) and (d) represent the HfSnSe$_3$ monolayers, (e) and (f) represent the HfSnTe$_3$ monolayers.

Fig. S2. AIMD simulations at room temperature for PP and FP HfSnX$_3$ monolayers. (a) and (b) represent the HfSnS$_3$ monolayers, (c) and (d) represent the HfSnSe$_3$ monolayers, (e) and (f) represent the HfSnTe$_3$ monolayers.
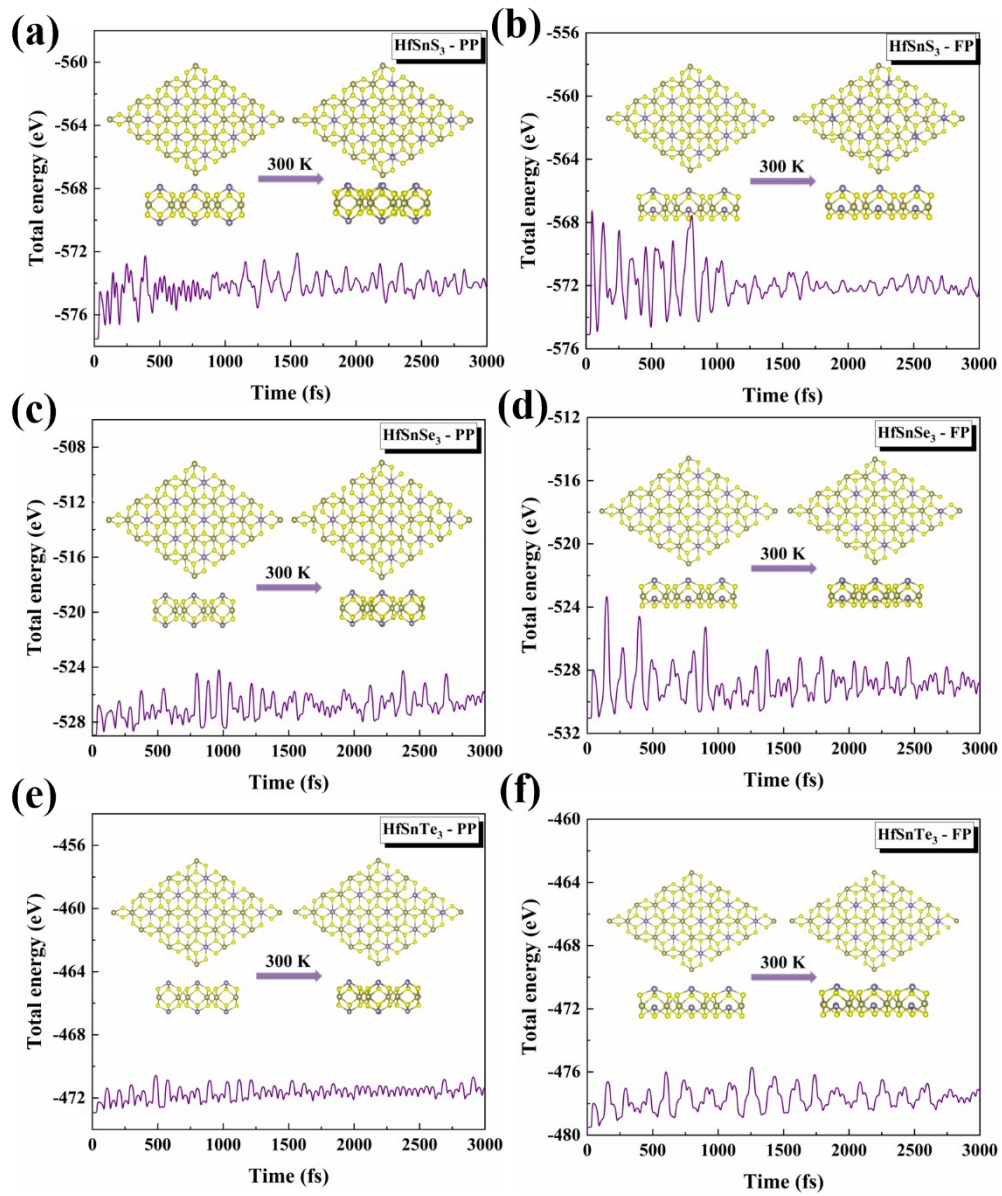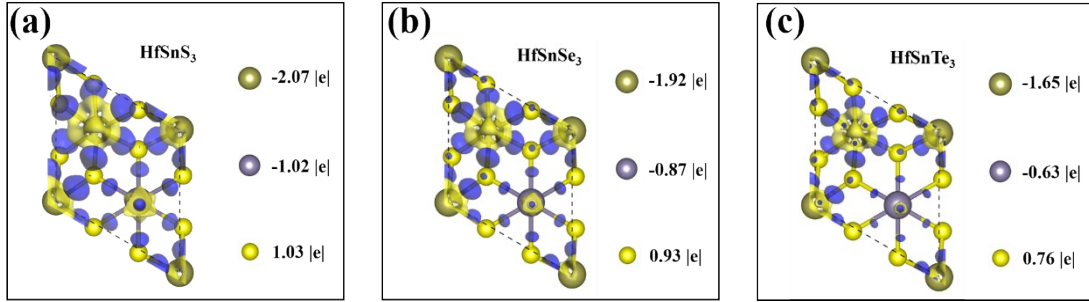
Fig. S3. Bader charges of (a) PP HfSnS$_3$ monolayers, (b) PP HfSnSe$_3$ monolayers and (c) PP HfSnTe$_3$ monolayers.
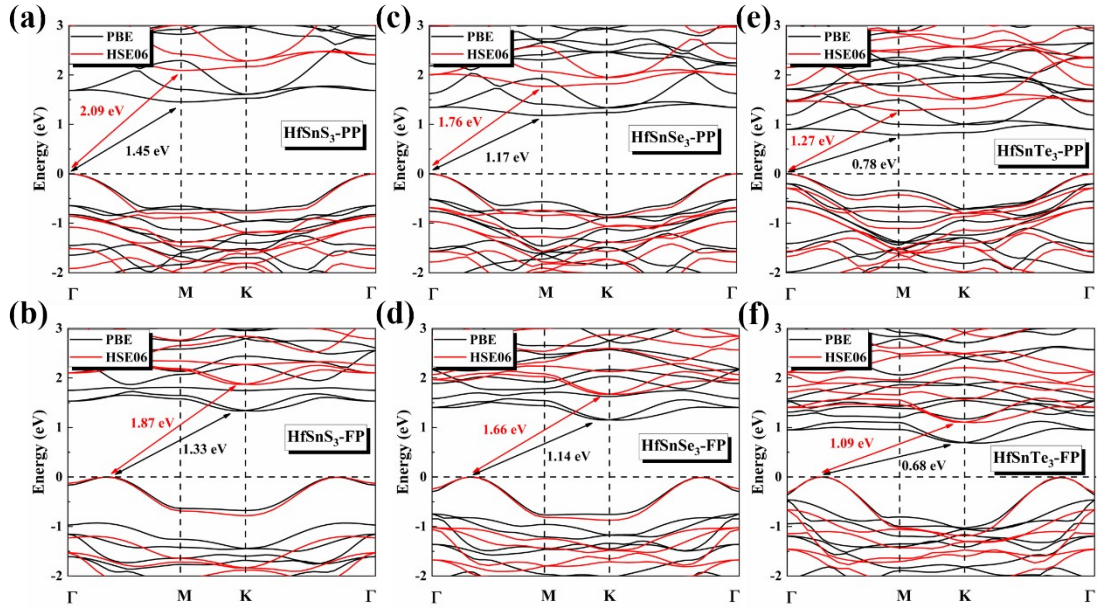

Fig. S4. Band structures of HfSnX$_3$ monolayers calculated by PBE and HSE06 functional (the VBM is set to zero). The Γ, M and K points in the first Brillouin zone are set as (0, 0, 0), (0.5, 0, 0) and (0.333, 0.333, 0), respectively.
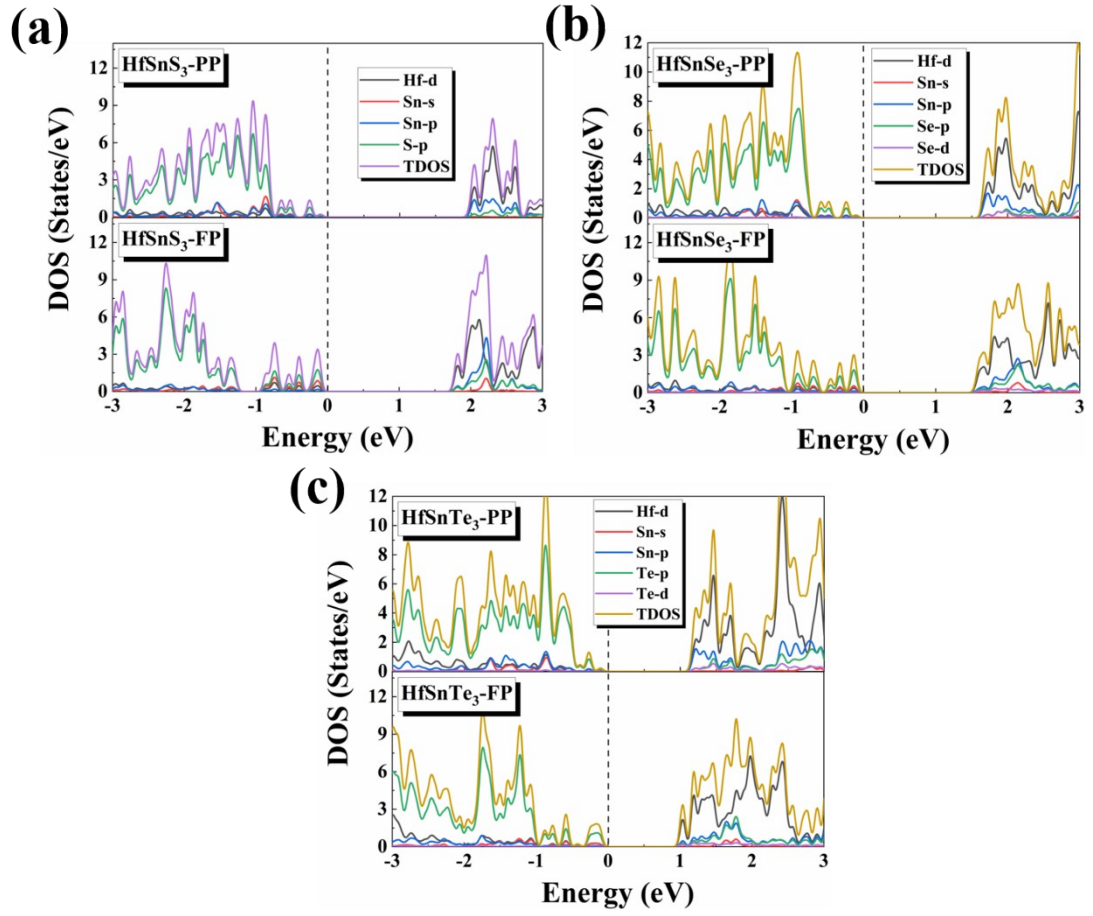
Fig. S5. (a), (b) and (c) are the orbital projection density of states of six HfSnX$_3$ monolayers using the HSE06 functional.
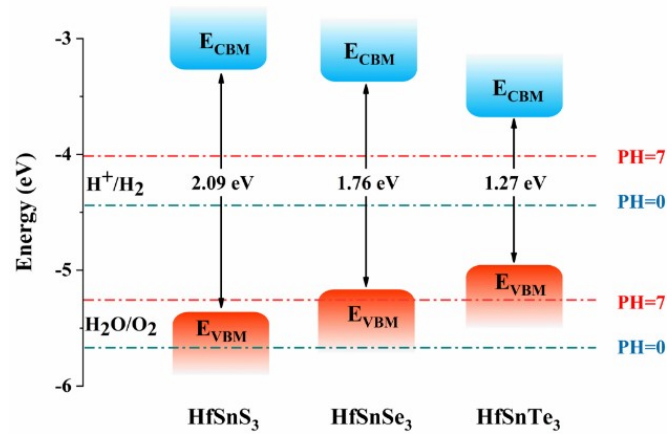

Fig. S6. Band edges of PP HfSnX$_3$ monolayers versus the redox potentials of water at pH = 0 and 7.
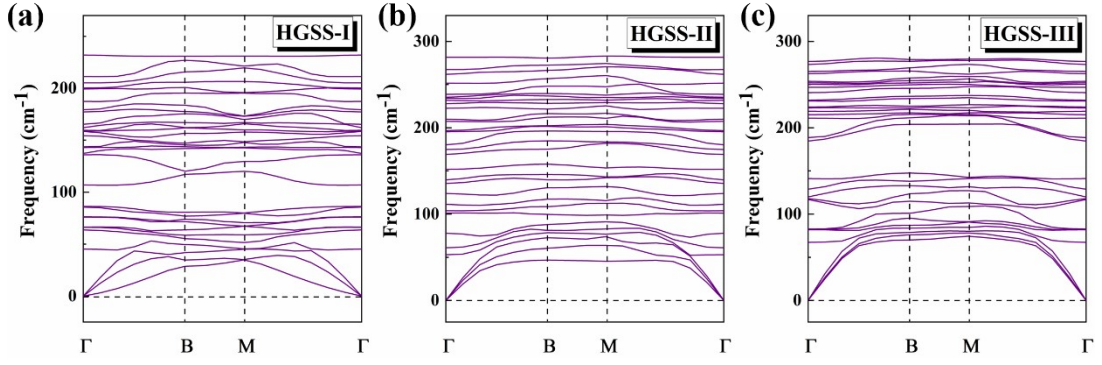
Fig. S7. Phonon spectrum of Janus HGSS monolayers. (a), (b) and (c) correspond to the HGSS-I, HGSS-II and HGSS-III, respectively.
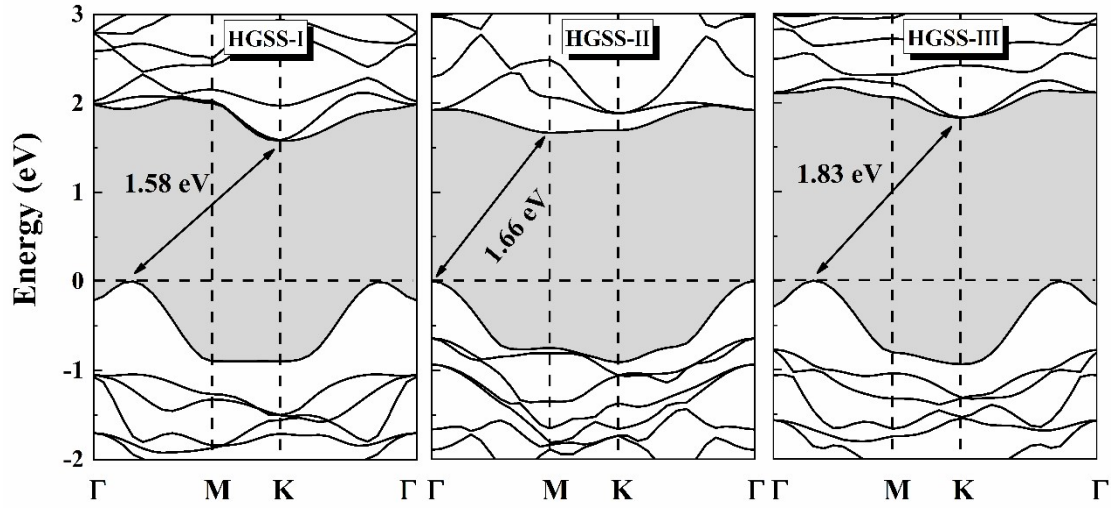

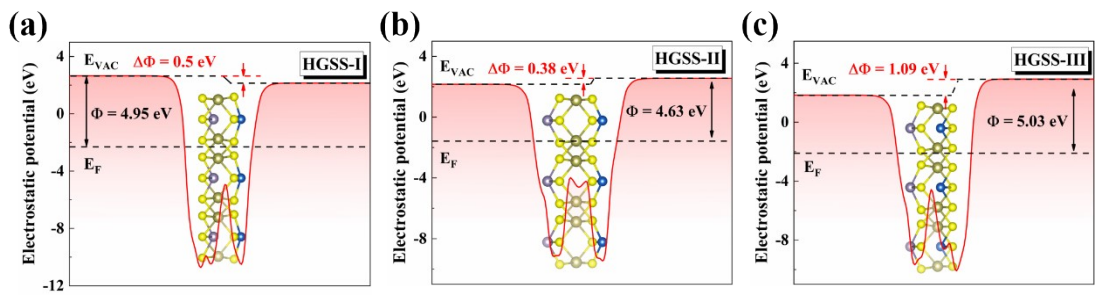**Figure S8** The band structures of HGSS monolayers calculated by HSE06 method.

Fig. S9. (a), (b) and (c) are the electrostatic potentials of the HGSS-I, HGSS-II and HGSS-III, respectively.
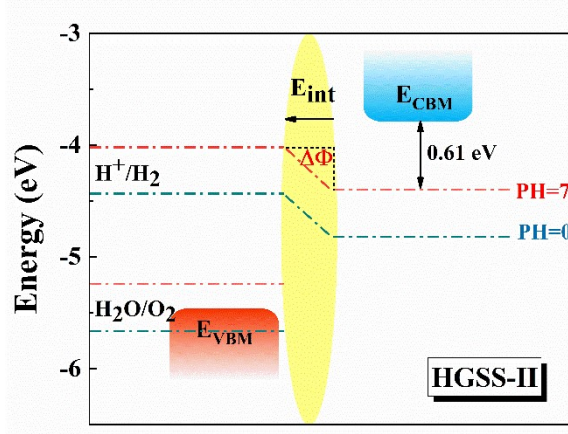
Fig. S10. The band arrangements of HGSS-II monolayers versus the redox potentials of water at pH = 0 and 7.

Calculation details of light absorption coefficient

The light absorption coefficient $\alpha(\omega)$ can be expressed as [1]:

$$\alpha(\omega) = \frac{\sqrt{2}\omega}{c}\left[\sqrt{\varepsilon_1^2(\omega) + \varepsilon_2^2(\omega)} - \varepsilon_1(\omega)\right]^{\frac{1}{2}} \tag{S1}$$

where the ε_1 and ε_2 are the real part and imaginary part of the dielectric constant, respectively, which defined as:

The light absorption coefficient $\alpha(\omega)$ can be obtained by $\varepsilon_1(\omega)$ and $\varepsilon_2(\omega)$:

$$\varepsilon_1(\omega) = 1 + \frac{2}{\pi}P\int_0^\infty \frac{\omega'\varepsilon_2(\omega)}{(\omega')^2 - \omega^2 + i\eta}d\omega' \tag{S2}$$

where P is the principle value. η denotes the complex shift in the Kramers-Kronig transformation

$$\varepsilon_2(\omega) = \frac{4\pi^2 e^2}{\Omega}\lim_{q\to 0}\frac{1}{q^2}\sum_{c,v,k}2\omega_k\delta(\varepsilon_{ck} - \varepsilon_{vk} - \omega) \times \left\langle\mu_{ck+e_{aq}}|\mu_{vk}\right\rangle\left\langle\mu_{ck+e_{aq}}|\mu_{vk}\right\rangle^* \tag{S3}$$

where the c and v refer to the conduction and valence band states, and Ω represents the volume of unit cell. The eigenvalues and eigenstates of the wave vector k in CB are represented by ε_{ck} and μ_{ck}, and the corresponding eigenvalues in VB are ε_{vk} and μ_{vk}, respectively.

The solar-to-hydrogen (STH) efficiency

STH efficiency is estimated by the product of the efficiency of light absorption η_{abs} and carrier utilization η_{cu} using the following expression [2,3]

$$\eta_{STH} = \eta_{abs} \times \eta_{cu} \tag{S4}$$

The efficiency of light absorption is defined as:

$$\eta_{abs} = \frac{\int_{E_g}^{\infty} P(h\omega)d(h\omega)}{\int_{0}^{\infty} P(h\omega)d(h\omega)} \tag{S5}$$

where E_g is the band gap of photocatalyst and $P(h\omega)$ is the AM1.5 solar energy flux at the photon energy $h\omega$.

The efficiency of carrier utilization (η_{cu}) is estimated by

$$\eta_{cu} = \frac{\Delta G_{H_2O} \int_{E}^{\infty} \frac{P(h\omega)}{h\omega}d(h\omega)}{\int_{E_g}^{\infty} P(h\omega)d(h\omega)} \tag{S6}$$

where ΔG_{H_2O} is the free energy of water splitting (1.23 eV). E represents the photon energy that can be actually utilized in the process of water splitting, which can be defined as:

$$E = \begin{cases} E_g, & (\chi(H_2) \geq 0.2, \chi(O_2) \geq 0.6) \\ E_g + 0.2 - \chi(H_2), & (\chi(H_2) < 0.2, \chi(O_2) \geq 0.6) \\ E_g + 0.6 - \chi(O_2), & (\chi(H_2) \geq 0.2, \chi(O_2) < 0.6) \\ E_g + 0.8 - \chi(H_2) - \chi(O_2), & (\chi(H_2) < 0.2, \chi(O_2) < 0.6) \end{cases} \tag{S7}$$

where $\chi(H_2)$ and $\chi(O_2)$ represent the over potentials for HER and OER, respectively. Considering the energy loss during carrier migration between different materials, the required over potentials for HER and OER reactions are suggested to be 0.2 and 0.6 eV, respectively.

The intrinsic electric field does positive work for the electron-hole separation. Therefore, the corrected STH efficiency takes the following form [3]:

$$\eta_{STH}^{'} = \eta_{STH} \times \frac{\int\limits_{0}^{\infty} P(h\omega)d(h\omega)}{\int\limits_{0}^{\infty} P(h\omega)d(h\omega) + \Delta\Phi \int\limits_{E_g}^{\infty} \frac{P(h\omega)}{h\omega}d(h\omega)}$$

(S8)

where $\Delta\Phi$ is the vacuum level difference on the two respective surfaces of 2D monolayers.

Calculation details and results of carrier mobility

The carrier mobility can be obtained by the flowing formula[4]:

$$\mu = \frac{e\hbar^3 C_{2D}}{K_B T m^* m_d E_{2D}^2}$$

(S9)

where e and $\hbar$ are the electron charge and reduced Planck constant, respectively. k_B and T represent the Boltzmann constant and temperature (300 K), respectively. The m^* is effective mass of electrons and holes along different directions. m_d represents the average effective mass, which can be represented as $m_d = \sqrt{m_x^* m_y^*}$. The C_{2D} and E_{2D} are the in-plane stiffness and deformation potential constant, respectively

The effective mass m^*, in-plane stiffness C_{2D} and deformation potential constant E_{2D} can be expressed by:

$$m^* = \hbar^2 \left[\frac{\partial^2 E(k)}{\partial k^2} \right]^{-1}$$

(S10)

where the $E(k)$, as the function of the momentum k, represent the total energies.

$$C_{2D} = \frac{\partial^2 E}{\partial \delta^2} \cdot \frac{1}{S_0}$$

(S11)

where δ and S_0 denote the applied strain and the pristine superficial area, respectively.

$$E_{2D} = \frac{\partial E_{edge}}{\partial \delta}$$

(S12)

E_{2D} represents the variation of band edge (E_{edge}) for VBM and CBM with the change of strain.

Table S1 Effective carrier masses (m^*), in-plane stiffness C_{2D}, deformation potential constant

E_{2D} and carrier mobility in HGSS-I monolayer.

direction	carrier type	m^*/m_0	C_{2D} (N m^{-1})	E_{2D} (eV)	μ (cm^2 V^{-1} s^{-1})
x	electron	0.75	2.46	0.55	308
	hole	0.20	2.46	-2.25	259
y	electron	0.75	2.66	0.99	103
	hole	0.20	2.66	-3.88	94

References

1. J. Liu, Y. Shen, X. Gao, L. Lv, Y. Ma, S. Wu, X. Wang and Z. Zhou, Applied Catalysis B-Environmental, 2020, **279**, 119368.

2. L. Ju, J. Shang, X. Tang and L. Kou, Journal of the American Chemical Society, 2020, **142**, 1492-1500.

3. C.-F. Fu, J. Sun, Q. Luo, X. Li, W. Hu and J. Yang, Nano Letters, 2018, **18**, 6312-6317.

4. X. Cai, Y. Chen, B. Sun, J. Chen, H. Wang, Y. Ni, L. Tao, H. Wang, S. Zhu, X. Li, Y. Wang, J. Lv, X. Feng, S. A. T. Redfern and Z. Chen, Nanoscale, 2019, **11**, 8260-8269.